

Spectroscopic investigation of photophysics and tautomerism of amino- and nitroporphycenes

Idaresit Mbakara,¹ Agnieszka Gajewska,¹ Arkadiusz Listkowski,^{1,2} Michał Kijak,¹ Krzysztof Nawara,^{1,2} Tatu Kumpulainen,^{3,4} Eric Vauthey,³ Jacek Waluk^{1,2}

¹Institute of Physical Chemistry, Polish Academy of Sciences, 01-224 Warsaw, Kasprzaka 44/52, Poland; ²Faculty of Mathematics and Science, Cardinal Stefan Wyszyński University, Dewajtis 5, 01-815 Warsaw, Poland; ³Physical Chemistry Department, Sciences II, University of Geneva, 30, Quai Ernest Ansermet, CH-1211 Geneva 4, Switzerland; ⁴Present address: Department of Chemistry/Nanoscience Center, University of Jyväskylä, Surfontie 9 C, 40014, Jyväskylä, Finland

Supporting information

Syntheses.....	2
Spectral and photophysical measurements.....	4
Purification by HPLC.....	4
Calculations.....	5
Figures.....	7

Syntheses

9-aminoporphycene (APc). The compound was obtained following a method known from the literature.¹ A solution of 24.5 mg (0.07 mmol) of 9-nitroporphycene in 25 ml dichloromethane was mixed with 10 ml of an aqueous 10% sodium hydroxide solution. To the reaction mixture were added 2.4 g (13.8 mmol) of sodium dithionite Na₂S₂O₄ and it was heated under reflux for 4 h (TLC *n*-hexane/ethyl acetate 2:1, silica gel). The color of the mixture changed from blue-green to deep blue. After cooling to room temperature and separating the two phases, the organic layer was washed three times with water, dried with sodium sulfate and the solvent was evaporated under vacuum. Chromatography on silica gel column with hexane/ethyl acetate 2:1 yielded 5 mg (22%) of the amino compound as a dark blue powder.

¹H NMR (500 MHz, CDCl₃) 9.52 (d, J = 10.9 Hz, 1H), 9.36 (dd, J = 6.0 Hz, J = 4.6 Hz, 2H), 9.34 – 9.29 (m, 2H), 9.27 (d, J = 10.9 Hz, 1H), 8.95 (m, 2H), 8.9 (d, J = 4.3 Hz, 1H), 8.86 (s, 1H), 8.83 (d, J = 4.3 Hz, 1H), 5.86 (bs, 2H), 5.35 (bs, 1H), 5.22 (bs, 1H);

HRMS (ESI⁺): m/z calcd for [M + H⁺] C₂₀H₁₆N₅: 326.1406; found: 326.1408.

9-amino-2,7,12,17-tetra-*n*-propylporphycene (tprAPc)

The compound was synthesized exactly according to the previously reported patent procedure.² Starting from 239 mg (0.5 mmol) of tetra-*n*-propylporphycene the title compound was obtained in the amount 160 mg (0.325 mmol) as a dark blue powder; 65% yield.

¹H NMR (400 MHz, CDCl₃), δ 9.48 (d, J = 11.1 Hz, 1H), 9.18 (d, J = 11.1 Hz, 1H), 9.04 (s, 1H), 9.03 (s, 1H), 9.02 (s, 2H), 8.67 (s, 1H), 5.71 (bs, 1H), 5.35 (bs, 1H), 4.94 (bs, 1H), 3.94 – 3.82 (m, 4H), 3.79 (t, J = 7.8 Hz, 2H), 3.73 (t, J = 7.6 Hz, 2H), 2.49 – 2.23 (m, 8H), 1.41 – 1.21 (m, 12H).

HRMS (ESI⁺): m/z calcd for [M + H⁺] C₃₂H₄₀N₅: 494.3284; found : 494.3288.

9-nitroporphycene (NPc). The compound was obtained using a previously published procedure.¹ 36 mg (0.116 mmol) of porphycene were dissolved in 36 ml 1,2-dichloroethane and 36 ml glacial acetic acid and combined with 1.44 g of AgNO₃. The stirred suspension was heated in oil bath up to 75°C; color change was visible (from violet to blue-green). The reaction could be followed by means of TLC (*n*-hexane/ethyl acetate 4:1, silica gel). After cooling to room temperature, the insoluble material was removed and the solution was brought to pH 6 - 6.5 with 10% aqueous K₂CO₃, washed twice with water, dried with sodium sulfate and the solvent was evaporated. Chromatography on silica gel column with hexane/ethyl acetate 4:1 yielded 24,5 mg (55,7%) of the nitro compound, as a dark blue powder.

¹H NMR (500 MHz, CDCl₃) δ 10.61 (s, 1H), 9.79 (d, J = 10.8 Hz, 1H), 9.69 (d, J = 10.7 Hz, 1H), 9.57 (d, J = 4.7 Hz, 1H), 9.55 – 9.47 (m, 4H), 9.24 (d, J = 4.5 Hz, 1H), 9.17 (d, J = 4.3 Hz, 1H), 9.14 (d, J = 4.4 Hz, 1H), 3.68 (bs, 1H), 3.03 (bs, 1H).

HRMS (ESI⁺): m/z calcd for [M + H⁺] C₂₀H₁₄N₅O₂: 356.1147; found: 356.1146.

9-nitro-2,7,12,17-tetra-*n*-propylporphycene (tprNPc)^{1,2}

The compound was synthesized exactly as described previously in a patent procedure.² Starting from 239 mg (0.5 mmol) tetra-*n*-propylporphycene, **tprNPc** was obtained in the amount of 210 mg (0.4254 mmol) as a dark blue powder; 85% yield.

¹H NMR (400 MHz, CDCl₃) δ 9.94 (s, 1H), 9.67 (d, *J* = 10.9 Hz, 1H), 9.62 (d, *J* = 10.9 Hz, 1H), 9.29 (d, *J* = 0.8 Hz, 1H), 9.24 (d, *J* = 0.9 Hz, 1H), 9.22 (d, *J* = 0.9 Hz, 1H), 9.16 (d, *J* = 0.7 Hz, 1H), 4.01 – 3.92 (m, 5H), 3.78 – 3.68 (m, 3H), 2.88 (bs, NH, 1H), 2.45 – 2.29 (m, 8H), 1.42 (bs, NH, 1H), 1.37 – 1.28 (m, 12H).

HRMS (ESI⁺): *m/z* calcd for [M + H⁺] C₃₂H₃₈N₅O₂ : 524.3026; found : 524.3026.

9-Nitro-2,7,12,17-tetra-*tert*-butylporphycene (ttNPc). 2,7,12,17-Tetra-*tert*-butylporphycene (100 mg, 0.186 mmol) was dissolved in a mixture of dichloromethane (40 mL) and acetic acid (40 mL). Then silver nitrate (2.96 g, 34.8 mmol) was added, and the mixture was stirred at room temperature for 25 min. After this time the reaction mixture was partitioned between water (300 mL) and dichloromethane (400 mL). The organic phase was washed with water (300 mL), then with 10% NaOH solution (250 mL), dried and concentrated. The expected product was isolated by column chromatography (hexanes/toluene/dichloromethane: 750/200/50) to give **ttNPc** (89 mg, 0.154 mmol, 83%) as a green solid.

¹H NMR (400 MHz, CDCl₃) δ 10.74 (s, 1H, H-10), 9.97 (AB, *J* = 11.3 Hz, 1H, H-19 or H-20), 9.88 (AB, *J* = 11.3 Hz, 1H, H-19 or H-20), 9.31 (s, 1H, H-6), 9.22 (s, 1H, H-13 or H-16), 9.20 (s, 1H, H-3), 9.14 (s, 1H, H-13 or H-16), 5.04 (s, 1H, NH), 3.72 (s, 1H, NH), 2.20 (s, 9H, H-12'), 2.19 (s, 9H, H-13' or H-16'), 2.18 (s, 9H, H-13' or H-16'), 1.95 (s, 9H, H-7'); ¹³C NMR (100 MHz, CDCl₃) δ 156.25, 155.82, 154.34, 149.84, 144.97, 144.16, 139.08, 138.02, 137.60, 136.49, 135.59, 133.67, 131.77, 126.36 (C-6), 123.50 (C-3), 122.38 (C-13 or C-16), 121.38 (C-13 or C-16), 116.11 (C-19 or C-20), 113.17 (C-19 or C-20), 108.83 (C-10), 35.63, 34.36, 34.21, 34.12, 33.80, 33.64, 33.47, 31.43, 30.19, 29.69. HRMS (ESI): *m/z* calculated for C₃₆H₄₆N₅O₂: 580.3652 [M+H]⁺; found: 580.3655.

9-Amino-2,7,12,17-tetra-*tert*-butylporphycene (ttAPc). 9-Nitro-2,7,12,17-tetra-*tert*-butylporphycene (**ttNPc**, 80 mg, 0.138 mmol) was dissolved in dichloromethane (50 mL). Then, 10% aqueous solution of NaOH (20 mL) was added, followed by the addition of sodium dithionite (4.8 g; 27.6 mmol). The mixture was stirred under reflux for 4 h. It was then cooled to room temperature and the reaction mixture was partitioned between dichloromethane (200 mL) and water (250 mL). The organic layer was washed with water (250 mL), dried and concentrated under reduced pressure. The expected product was isolated by column chromatography (alumina, hexanes/ethyl acetate: 18/1) as a blue solid (**ttAPc**, 40 mg, 0.073 mmol, 53%).

¹H NMR (400 MHz, CDCl₃) δ 9.85 (AB, *J* = 11.6 Hz, 1H, H-19 or H-20), 9.52 (AB, *J* = 11.6 Hz, 1H, H-19 or H-20), 9.26 (s, 1H, H-3 or H-16), 9.22 (s, 1H, H-10), 9.10 (d, *J* = 0.8 Hz, 1H, H-3 or H-16), 9.08 (s, 1H, H-4 or H-13), 9.06 (s, 1H, H-4 or H-13), 6.05 (s, 2H, NH₂), 5.87 (s, 1H, H-21 or H-24), 5.36 (s, 1H, H-22 or H-23), 2.18 (s, 9H, H-2' or H-17'), 2.15 (s, 9H), 2.15 (s, 18H); ¹³C NMR (100 MHz, CDCl₃) δ 153.55, 152.12, 150.98, 148.30, 144.55, 144.48, 139.45, 138.45, 134.30, 132.41, 131.80, 131.74, 131.27 (C^{IV}), 123.08, 122.25, 121.81, 119.75,

115.59 (C-19 or C-20), 109.25 (C-19 or C-20), 103.93 (C-10), 34.13 ($\underline{C}(\text{CH}_3)_3$), 34.03 ($\underline{C}(\text{CH}_3)_3$), 33.99 ($\underline{C}(\text{CH}_3)_3$), 33.78 ($\underline{C}(\text{CH}_3)_3$), 33.60 ($\underline{C}(\text{CH}_3)_3$), 33.43 ($\underline{C}(\text{CH}_3)_3$), 33.42 ($\underline{C}(\text{CH}_3)_3$), 32.28 ($\underline{C}(\text{CH}_3)_3$). HRMS (ESI): m/z calculated for $\text{C}_{36}\text{H}_{48}\text{N}_5$: 550.3910 $[\text{M}+\text{H}]^+$; found: 550.3909.

Purification by HPLC

The HPLC was performed using a SHIMADZU LC-20AT Liquid Chromatograph equipped with SPD-20AV UV-vis detector, SIL-20AC autosampler, and FRC-10A fraction collector. The purification was achieved using Phenomenex Luna 5 μm C18(2) 100 Å (250x10 mm) column. The mobile phase consisted of ultrapure water and acetonitrile, at a ratio of 20:80. The samples were filtered through 0.45 μm PTFE filters before HPLC.

Spectral and photophysical measurements

Electronic absorption spectra were measured on a Shimadzu UV2700 spectrophotometer. Solvents (acetonitrile, *n*-hexane, toluene, and paraffin oil, all from Merck) were of spectral grade and they were used as supplied.

Stationary fluorescence and excitation spectra were recorded on an Edinburgh FS 900 CDT spectrofluorimeter, Cary Eclipse fluorescence spectrometer, and Fluorolog or FluoroMax-4, both from Horiba Jobin Yvon. The fluorescence quantum yields were determined at room temperature for non-deaerated samples, using parent porphycene³ as a reference.

Magnetic circular dichroism (MCD) spectra were recorded with Jasco J-1500 CD spectrometer, equipped with an electromagnet (1.36 T field strength).

Fluorescence lifetimes were obtained using a home-built setup. Fianium FemtoPower1060 laser served as a wavelength-tunable excitation source (6 ps pulse width, pulse energy of 1.6 nJ, repetition rate of 10/20/40/60 MHz). The emission was collected by a Digikröm CM112 double grating monochromator working in a subtractive mode. The optical

signal from the monochromator was detected by an HPM-100-40 hybrid detector (Becker & Hickl) coupled to a Becker & Hickl SPC-830 TR-SPC module. The FWHM of the instrument response function was 150 ps. Analysis of the decay profiles was performed using commercially available packages: SPCImage software, version 5.7 (Becker & Hickl) and FAST version 3.5.0 (Edinburgh Instruments). To make sure that reliable values are obtained in cases of non-singly exponential decays, two different procedures were used: (i) iterative reconvolution; (ii) distribution analysis.

Calculations

The molecular modeling of the studied systems has been performed using the Gaussian 16 suite of programs.⁴ The density functional theory (DFT) method with a hybrid B3LYP and its long-range corrected modification CAM-B3LYP functionals were chosen. The excited state energies were obtained in the framework of the time-dependent DFT (TD-DFT) approach. The Pople's split-valence 6-31+G** basis set was applied. The frequency analysis was performed for all stationary points. A vibrational frequency scaling factor of 0.964 was used to obtain zero-point vibrational energy (ZPVE) corrections.

Table S1. Calculated relative energies (kcal/mol) of the tautomeric forms of 2,7,12,17-tetra-*n*-propylporphycene (**tprPc**), 9-amino-2,7,12,17-tetra-*n*-propylporphycene (**tprAPc**), and 9-nitro-2,7,12,17-tetra-*n*-propylporphycene (**tprNPc**).

	S_0 ^a	S_1 ^b	$\mu(S_0)$ [D]	$\mu(S_1)$ ^{b,c} [D]
tprPc				
<i>trans</i>	0.00 (0.00)	0.00 (0.00)	0.06	0.04
		0.00 (0.00)		0.05
<i>cis</i>	2.27 (1.76)	1.85 (1.37)	1.40	1.07
		2.14 (1.41)		1.61
tprAPc				
<i>trans-1</i>	0.00 (0.00)	0.00 (0.00)	2.22	3.50
		0.00 (0.00)		2.98
<i>trans-2</i>	0.22 (0.15)	2.92 (2.20)	2.43	3.77
		2.59 (2.18)		3.23
<i>cis-1</i>	2.02 (1.48)	5.24 (4.02)	3.10	3.87
		5.23 (4.02)		3.70
<i>cis-2</i>	2.33 (1.70)	1.77 (1.39)	2.29	3.49
		1.91 (1.53)		3.45
tprNPc				
<i>trans-1</i>	0.06 (0.10)	0.29 (0.11)	6.11	7.57
		0.83 (0.67)		6.58
<i>trans-2</i>	0.00 (0.00)	0.00 (0.00)	6.27	8.16
		0.00 (0.00)		7.16
<i>cis-1</i>	2.44 (1.93)	1.98 (1.54)	6.09	7.84
		2.24 (1.67)		6.75
<i>cis-2</i>	1.83 (1.33)	2.13 (1.42)	6.66	7.82
		2.58 (1.75)		7.71

^a in parentheses, zero-point-corrected values; ^b first row, B3LYP/6-31+G(d,p), second row, CAM-B3LYP/6-31+G(d,p) results; ^c optimized S_1 geometries.

Table S2. Calculated transition energies (cm⁻¹) of the tautomeric forms of **tprPc**, **tprAPc**, and **tprNPc**.

	S ₁ ←S ₀ ^a	S ₁ →S ₀ ^b	S ₂ ←S ₀ ^a
tprPc			
<i>trans</i>	17534 (0.15) ^c	16480 (0.17) 16245 (0.23)	18589 (0.26)
<i>cis</i>	17484 (0.14)	16258 (0.16) 16271 (0.23)	18660 (0.24)
tprAPc			
<i>trans1</i>	16044 (0.21)	15077 (0.22) 14854 (0.27)	18668 (0.20)
<i>trans2</i>	16917 (0.30)	16056 (0.30) 15860 (0.40)	17866 (0.11)
<i>cis1</i>	17110 (0.25)	16257 (0.24) 16171 (0.37)	18173 (0.16)
<i>cis2</i>	15996 (0.21)	14763 (0.21) 14385 (0.27)	18240 (0.18)
tprNPc			
<i>trans1</i>	17126 (0.11)	14605 (0.12) 15326 (0.20)	17924 (0.17)
<i>trans2</i>	16854 (0.11)	15152 (0.12) 15365 (0.18)	18186 (0.25)
<i>cis1</i>	16794 (0.12)	14943 (0.13) 15225 (0.20)	18087 (0.23)
<i>cis2</i>	17008 (0.10)	15058 (0.11) 15765 (0.18)	18206 (0.14)

^a optimized S₀ geometry; ^b optimized S₁ geometry, first row: B3LYP/6-31G+(d,p), second row: CAM-B3LYP/6-31G+(d,p); ^c oscillator strength in parentheses

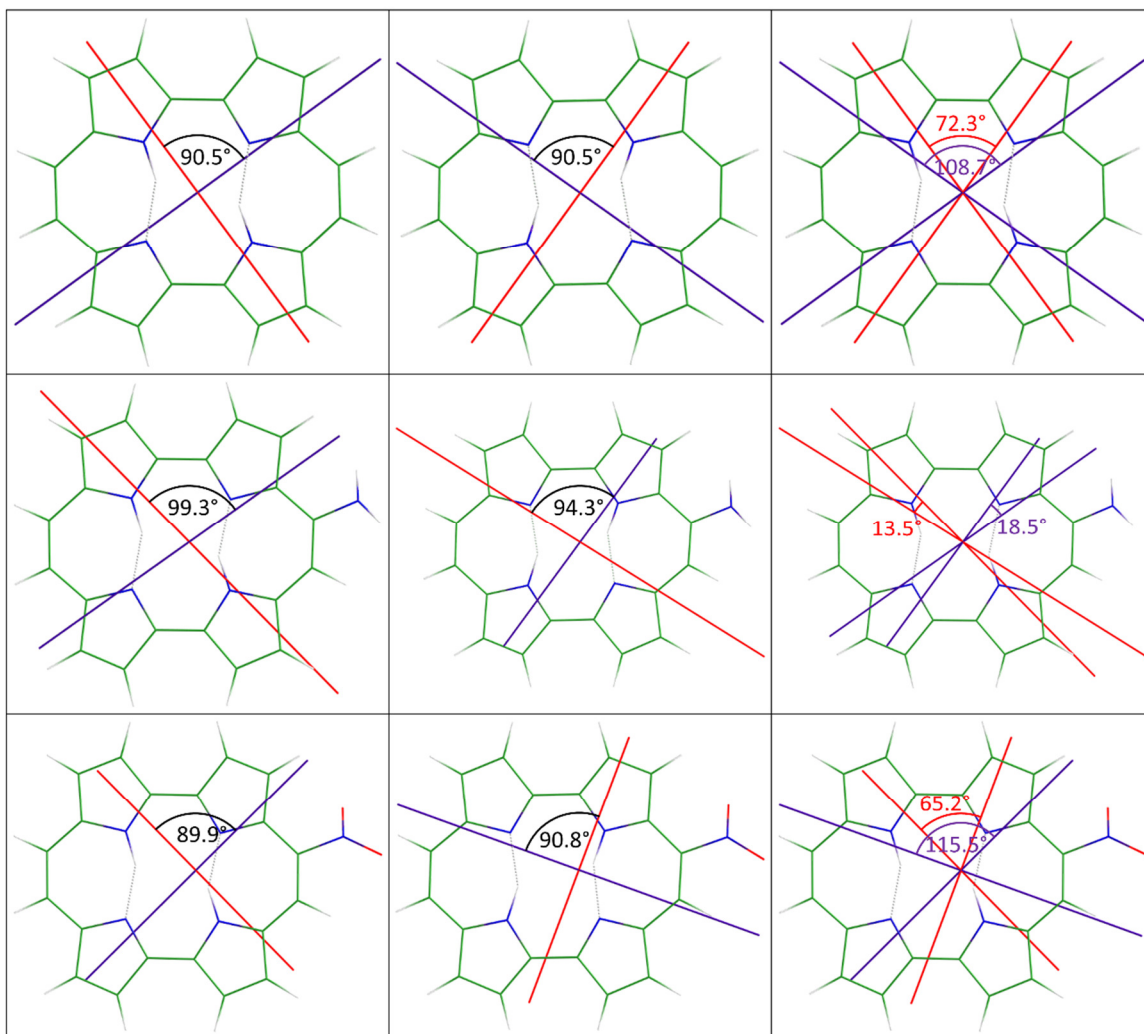


Figure S1. Calculated directions of $S_1 \leftarrow S_0$ (red) and $S_2 \leftarrow S_0$ (violet) transitions in **Pc** (top), **APc** (middle), and **NPc** (bottom) in the *trans1* (left column) and *trans2* (middle column) forms. The right column shows transition moment directions for both forms. The respective angles are marked in the drawings.

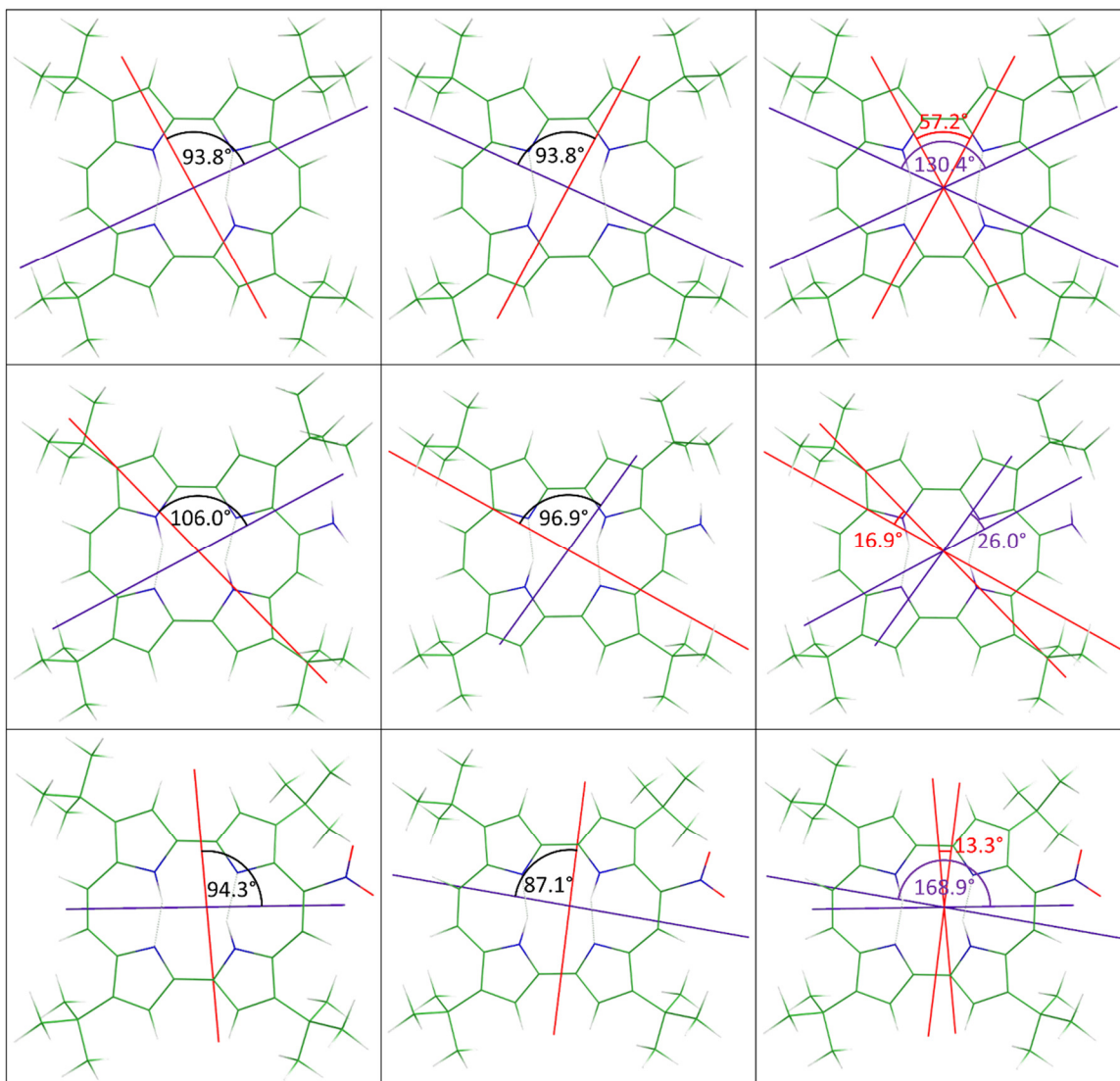


Figure S2. Calculated directions of $S_1 \leftarrow S_0$ (red) and $S_2 \leftarrow S_0$ (violet) transitions in **ttPc** (top), **ttAPc** (middle), and **ttNPc** (bottom) in the *trans1* (left column) and *trans2* (middle column) forms. The right column shows transition moment directions for both forms. The respective angles are marked in the drawings.

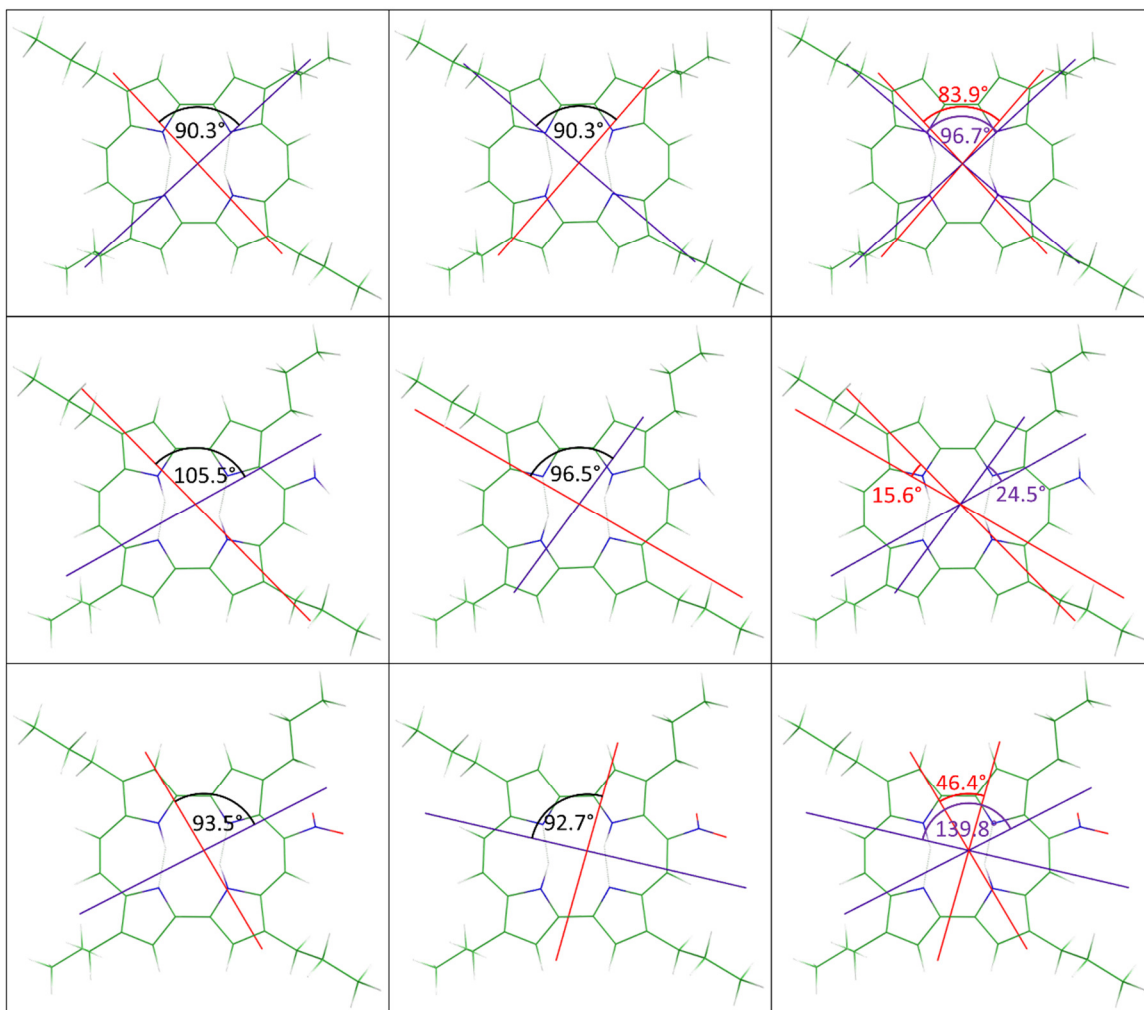


Figure S3. Calculated directions of $S_1 \leftarrow S_0$ (red) and $S_2 \leftarrow S_0$ (violet) transitions in **tprPc** (top), **tprAPc** (middle), and **tprNPc** (bottom) in the *trans1* (left column) and *trans2* (middle column) forms. The right column shows transition moment directions for both forms. The respective angles are marked in the drawings.

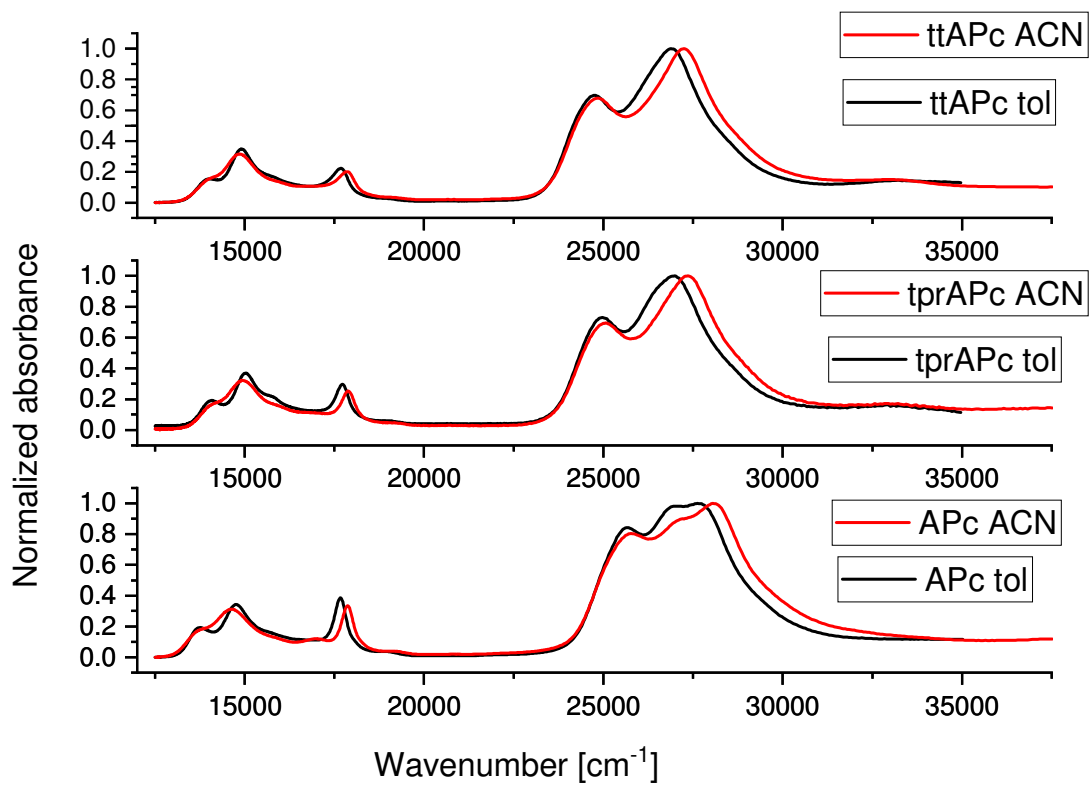


Figure S4. Absorption spectra of **APc** (bottom), **tprAPc** (middle), and **ttAPc** (top) in toluene (black) and acetonitrile (red).

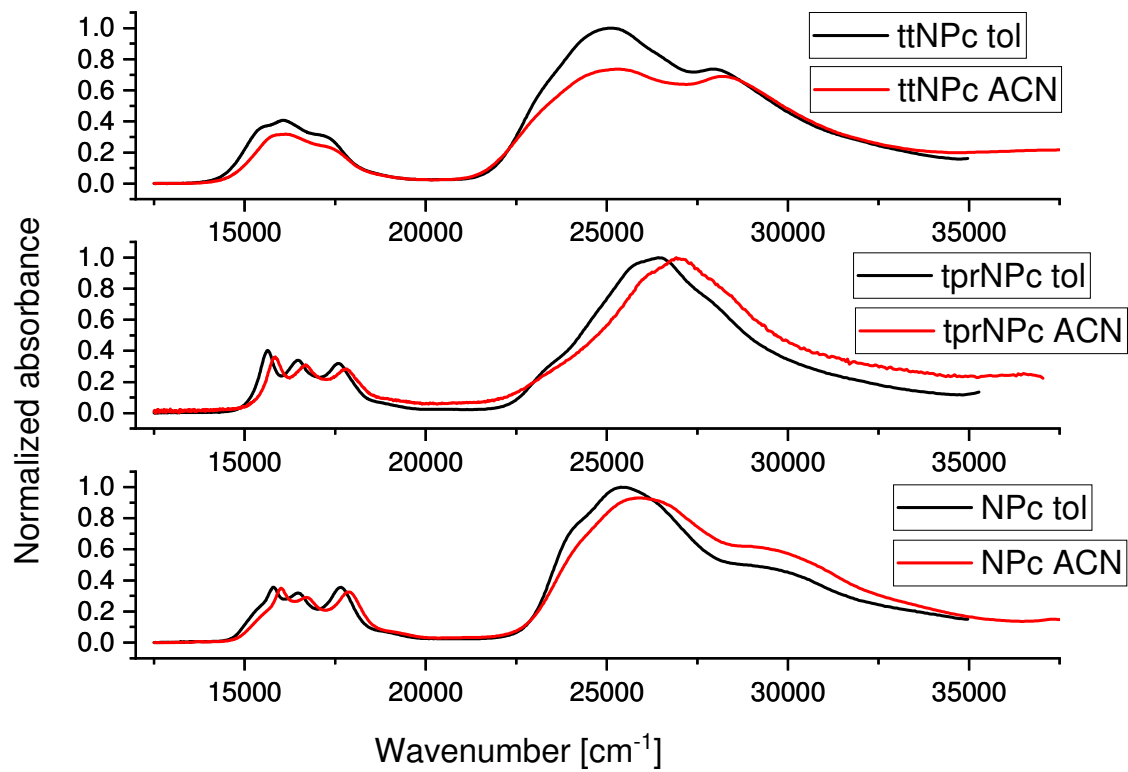


Figure S5. Absorption spectra of **NPc** (bottom), **tprNPc** (middle), and **ttNPc** (top) in toluene (black) and acetonitrile (red).

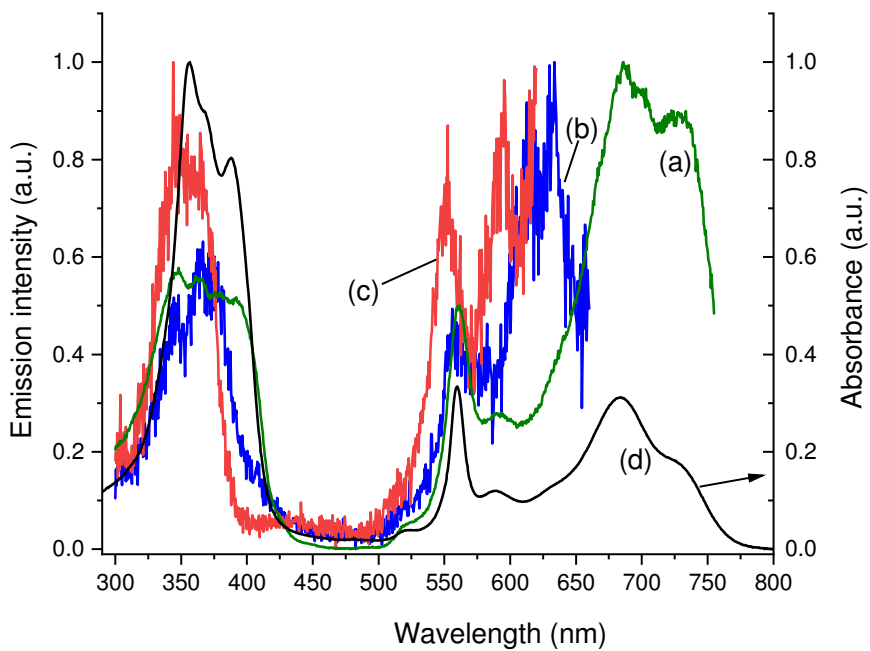


Figure S6. Fluorescence excitation spectra of **APc** in acetonitrile, taken several weeks after synthesis, monitored at 760 (a), 670 (b), and 630 nm (c). (d), absorption spectrum. The spectra were not corrected by the wavelength profile of the excitation beam.

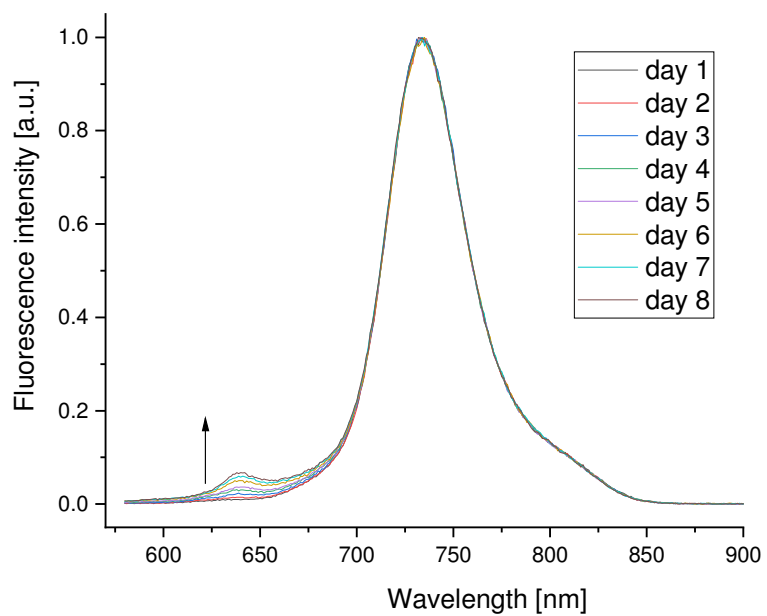


Figure S7. Fluorescence of a sample of **tprAPc** in acetonitrile recorded at one day intervals from the moment of synthesis. The arrow shows the increase of the band peaking at 640 nm. The excitation wavelength was 560 nm. The sample was stored in the dark between measurements.

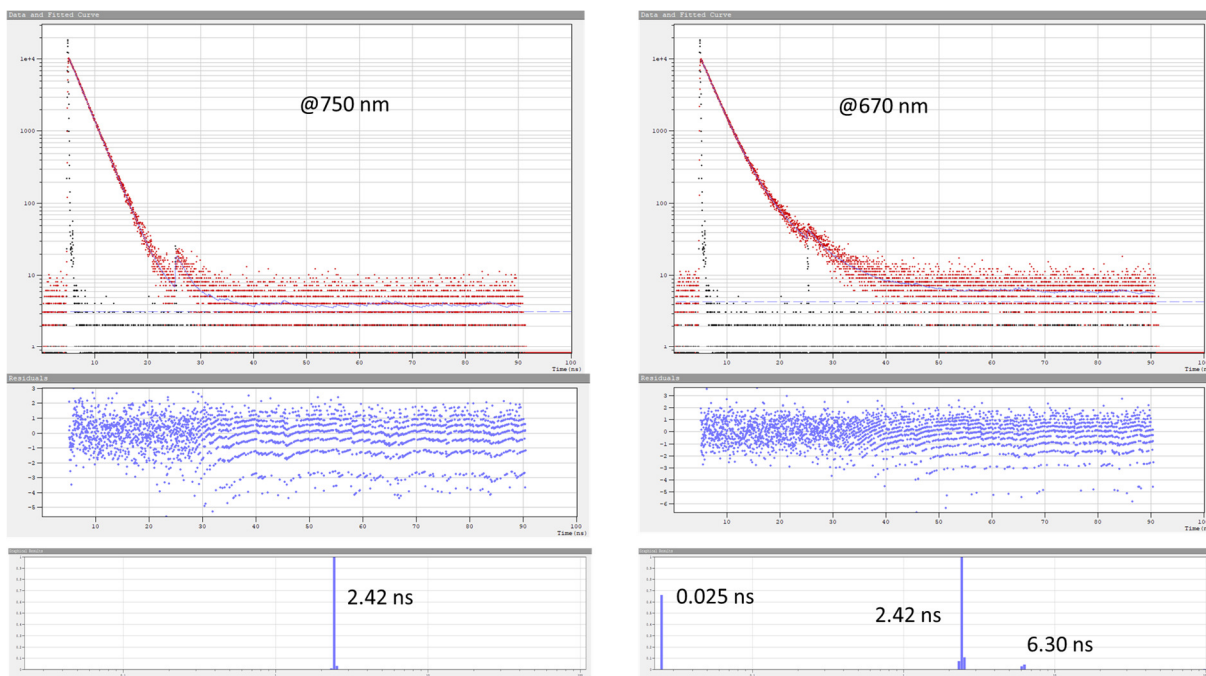


Figure S8. Top, emission decay kinetics of **tprAPc** in toluene. Fluorescence monitored at 750 nm (left) or 670 nm (right). Excitation wavelength: 552 nm. Bottom, results of distribution analysis. Middle: residuals. The 6.30 ns component is due to an impurity.

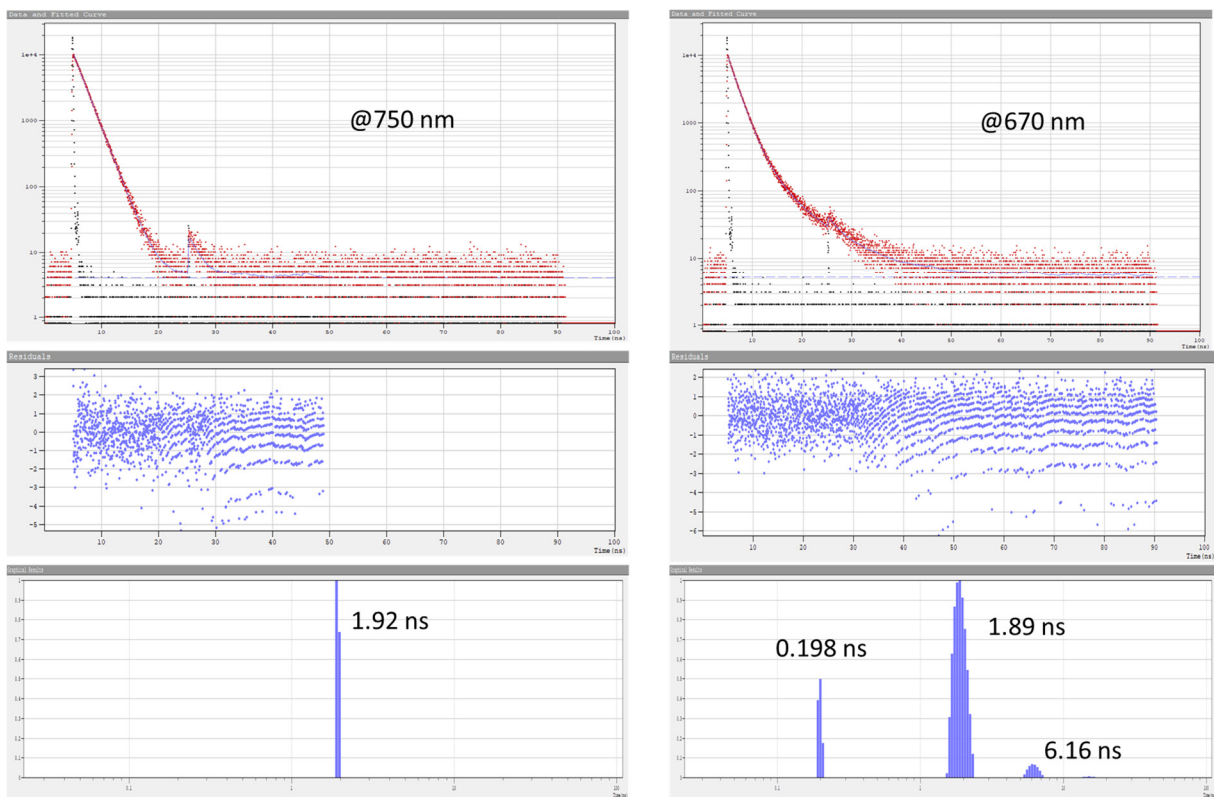


Figure S9. Top, emission decay kinetics of **tprAPc** in acetonitrile. Fluorescence monitored at 750 nm (left) or 670 nm (right). Excitation wavelength: 552 nm. Bottom, results of distribution analysis. Middle: residuals. The 6.16 ns component is due to an impurity.

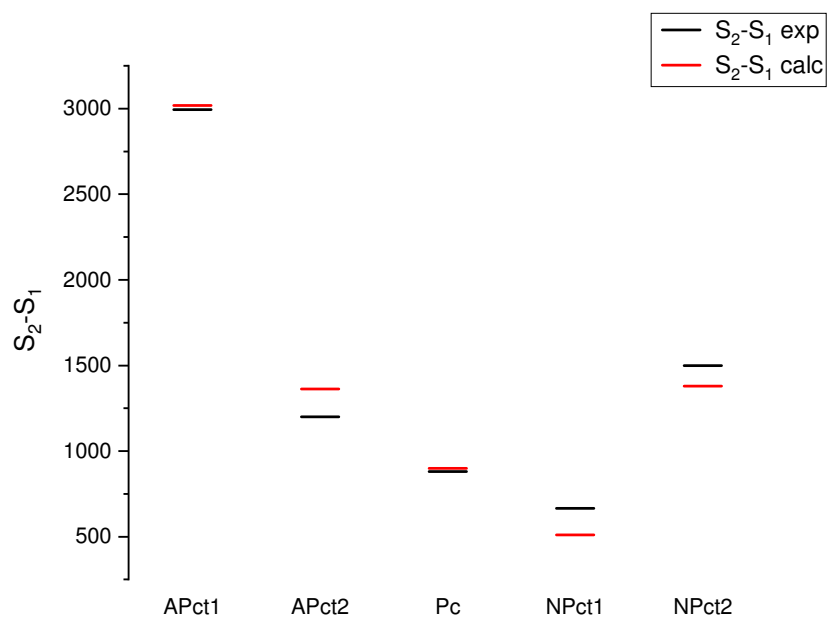


Figure S10. Experimental (black) and calculated (red) S₁-S₂ energy differences in **Pc**, **APc**, and **NPc**.

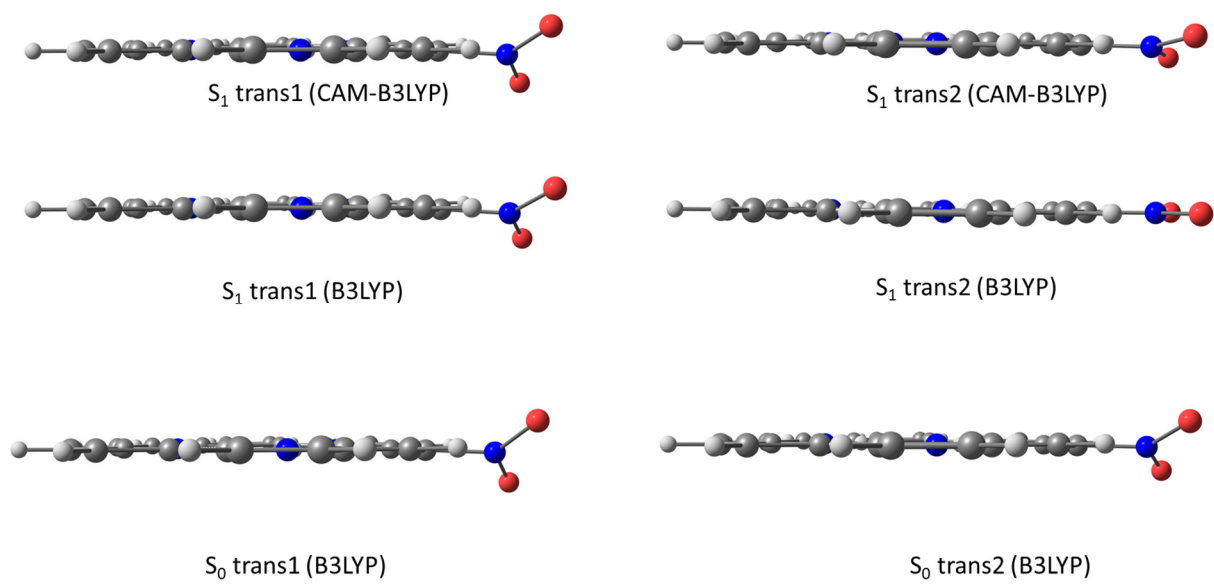
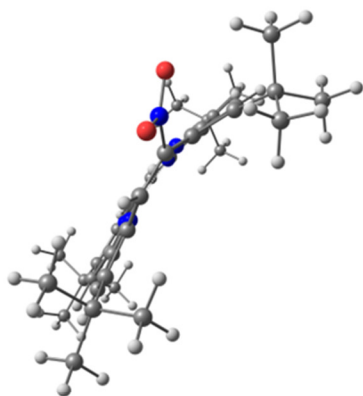
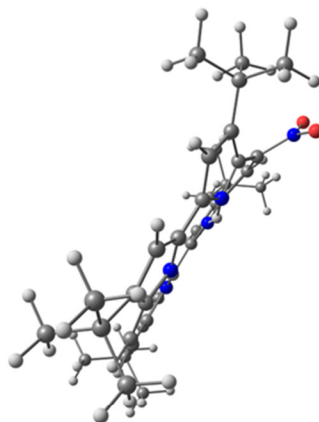


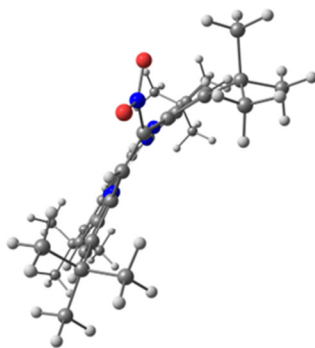
Figure S11. Optimized geometries of **NPc** in S_0 and S_1 states.



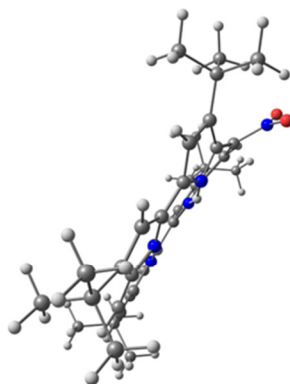
S_1 trans1 (CAM-B3LYP)



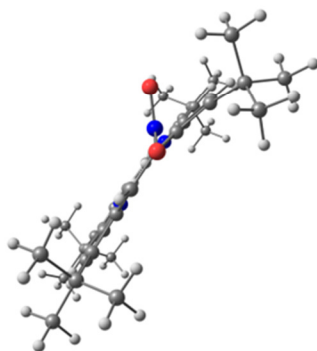
S_1 trans2 (CAM-B3LYP)



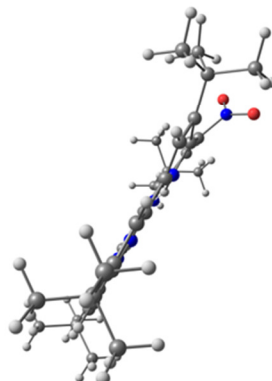
S_1 trans1 (B3LYP)



S_1 trans2 (B3LYP)

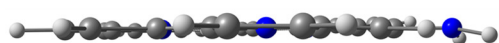


S_0 trans1 (B3LYP)



S_0 trans2 (B3LYP)

Figure S12. Optimized geometries of **ttNPc** in S_0 and S_1 states.



S_1 trans1 (CAM-B3LYP)



S_1 trans2 (CAM-B3LYP)



S_1 trans1 (B3LYP)



S_1 trans2 (B3LYP)

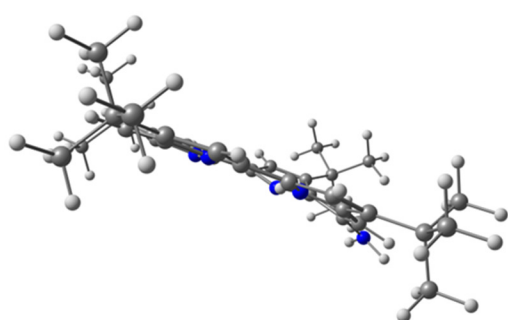


S_0 trans1 (B3LYP)

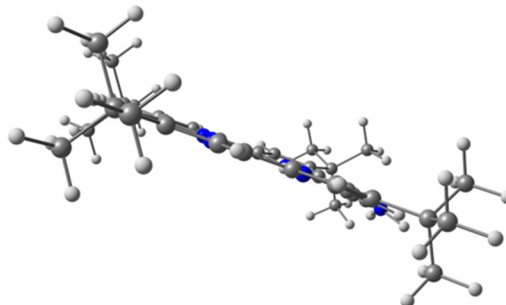


S_0 trans2 (B3LYP)

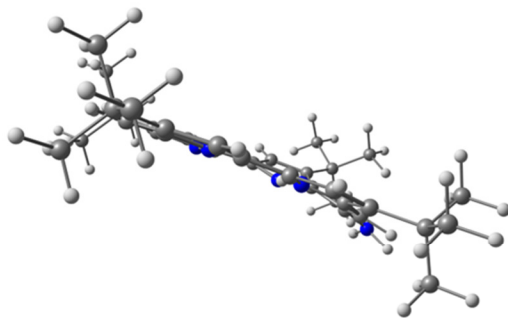
Figure S13. Optimized geometries of **APc** in S_0 and S_1 states.



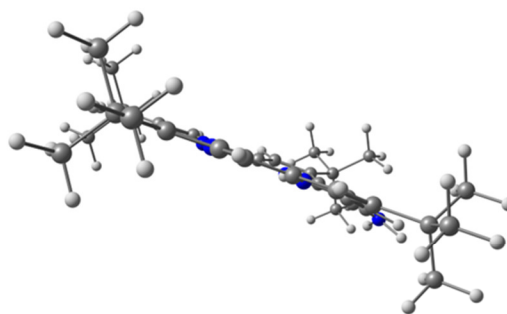
S_1 trans1 (CAM-B3LYP)



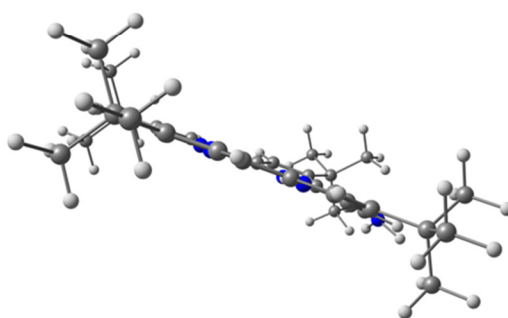
S_1 trans2 (CAM-B3LYP)



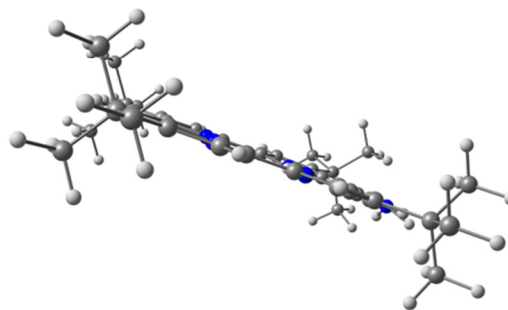
S_1 trans1 (B3LYP)



S_1 trans2 (B3LYP)



S_0 trans1 (B3LYP)



S_0 trans2 (B3LYP)

Figure S14. Optimized geometries of **ttAPc** in S_0 and S_1 states.

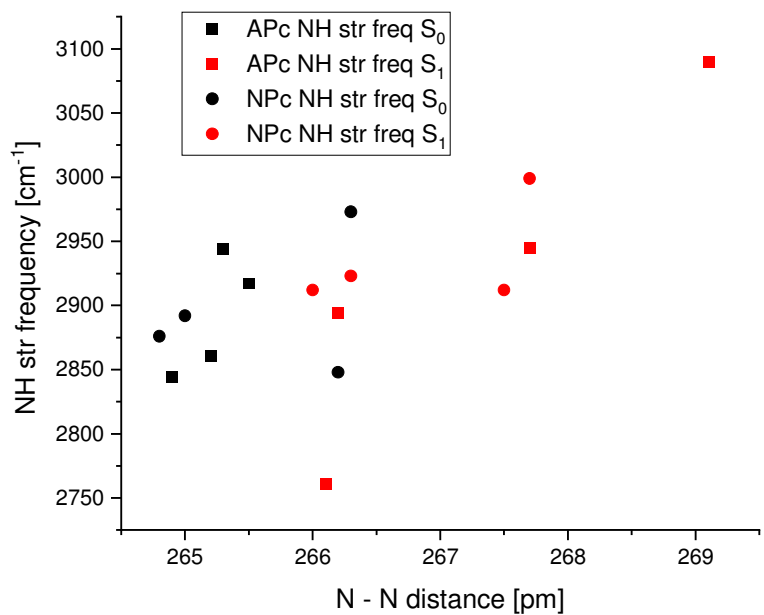


Figure S15. Correlation between the calculated NH stretching frequencies and the distances between nitrogen atoms engaged in the intramolecular hydrogen bonds.

References

- ¹ Vogel E., Koch P., Rahbar A., Cross A. Patent nr WO1992012636, **1992**.
- ² Vogel E., Mueller M., Halpen O., Cross A. Patent nr WO96/31451, **1996**.
- ³ Kijak, M.; Nawara, K.; Listkowski, A.; Masiera, N.; Buczyńska, J.; Urbańska, N.; Orzanowska, G.; Pietraszkiewicz, M.; Waluk, J.. *J. Phys. Chem. A* **2020**, *124*, 4594-4604.
- ⁴ Frisch, M.; Trucks, G.; Schlegel, H.; Scuseria, G.; Robb, M.; Cheeseman, J.; Scalmani, G.; Barone, V.; Petersson, G.; Nakatsuji, H.; Li, X.; Caricato, M.; Marenich, A.; Bloino, J.; Janesko, B.; Gomperts, R.; Mennucci, B.; Hratchian, H.; Ortiz, J.; Izmaylov, A.; Sonnenberg, J.; Williams-Young, D.; Ding, F.; Lipparini, F.; Egidi, F.; Goings, J.; Peng, B.; Petrone, A.; Henderson, T.; Ranasinghe, D.; Zakrzewski, V. G.; Gao, J.; Rega, N.; Zheng, G.; Liang, W.; Hada, M.; Ehara, M.; Toyota, K.; Fukuda, R.; Hasegawa, J.; Ishida, M.; Nakajima, T.; Honda, Y.; Kitao, O.; Nakai, H.; Vreven, T.; Throssell, K.; Montgomery, J. A. J.; Peralta, J.; Ogliaro, F.; Bearpark, M.; Heyd, J. J.; Brothers, E.; Kudin, K. N.; Staroverov, V. N.; Keith, T.; Kobayashi, R.; Normand, J.; Raghavachari, K.; Rendell, A.; Burant, J. C.; Iyengar, S. S.; Tomasi, J.; Cossi, M.; Millam, J. M.; Klene, M.; Adamo, C.; Cammi, R.; Ochterski, J. W.; Martin, R. L.; Morokuma, K.; Farkas, O.; Foresman, J.; Fox, D. *Gaussian 16, Revision B.01*, Gaussian, Inc., Wallingford CT: 2016.